# Design of OCSRR-Based Differential Microwave Sensor for Microfluidic Applications

Jianyuan Yu, Guohua Liu, Zhiqun Cheng, *Member, IEEE*, Yu Song, and Minghui You

***Abstract*—In this article, a high-sensitivity differential microwave sensor based on open comprehensive split-ring resonator (OCSRR) is proposed to extract the complex dielectric constant of liquid samples. An OCSRR structure is etched on the metal plate attached to the upper layer of the substrate. In addition, the outer ring of OCSRR adopts a hexagonal structure to reduce the original capacitance of OCSRR, and the inner ring of OCSRR adopts a rectangular structure to facilitate optimization and obtain the highest electric field intensity. The polydimethylsiloxane (PDMS) microfluidic channel is placed on the side of the outer ring with high electric field intensity and injects different concentrations of water–ethanol mixture. During resonance, the electric field is concentrated along the slit where the microfluidic channel is located. When the liquid sample is injected, the corresponding reflection coefficient changes. The designed sensor is fabricated and tested, and the experimental results are in good agreement with the simulation results. Compared with the previous similar sensors, the sensor can suppress the influence of environmental factors and has an average high sensitivity of 0.88%.**

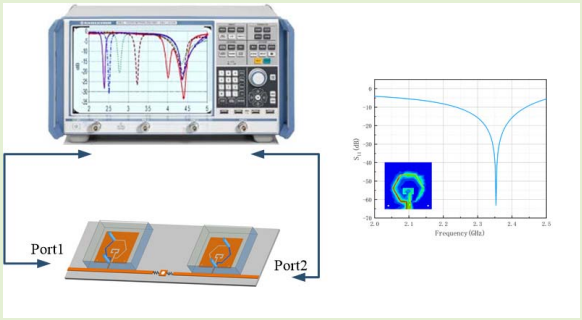


***Index Terms*— Differential measurement, high sensitivity, microfluidic sensor, open complementary split-ring resonator (OCSRR).**

## I. Introduction

IN RECENT ten years, microwave sensor, as a relatively reliable sensor, has been more and more widely used. In the aspect of medical biology, microwave sensors can detect the culture status of biological tissue [1], [2]. In environmental monitoring, a microwave sensor can be used to detect the temperature and humidity of the environment [3], [4]. In physics, microwave sensors can be used to retrieve parameters such as object displacement and rotation angle [5], [6]. In the aspect of industrial production, microwave sensors can be used to characterize the dielectric properties of solid and liquid chemicals [7], [8], [9]. Moreover, the microwave microfluidic sensor does not need labeling protocol or biomarker [10], which makes the study of liquid chemicals or biological liquids no longer need to consume a lot of reagents, solutions, and time, which greatly reduces the cost of liquid parameter extraction.

In microwave sensors, compared with cavity and dielectric resonance-based sensors, a planar resonance sensor is generally the first choice because it is easier to realize on-chip integration. Common structures in planar resonator sensors include split-ring resonators (SRRs) [11], [12], [13], [14], [15], complementary SRR (CSRR) [16], [17], [18], [19], open CSRR (OCSRR) [20], and so on. The electromagnetic properties of these particles depend on the dielectric constant of liquid under test (LUT). By measuring the resonant frequency and amplitude of the resonator loaded with LUT, the complex dielectric constant of LUT can be deduced inversely. Most of the recent improvements in planar resonator sensors have focused on improving sensitivity and reducing losses in the LUT. In [21], a microwave sensor with a CSRR loaded with a planar microwave probe is proposed. Compared with the traditional planar resonant sensor, the proposed single port structure can be directly immersed in the liquid sample and can easily measure the liquid dielectric constant. A structure in which three coupled dielectric sensing units are connected in series is proposed to enhance the sensitivity of the sensing area in [22]. To make the LUT completely cover the three sensing units to achieve the highest sensitivity, the sensor needs 400–1200-$\mu$L

Manuscript received 23 September 2022; accepted 29 September 2022. Date of publication 10 October 2022; date of current version 14 November 2022. This work was supported in part by the National Key R&D Program of China under Grant 2018YFE0207500, in part by the Project of Ministry of Science and Technology under Grant D20011, in part by the Zhejiang Provincial Public Technology Research Project under Grant LGG21F010006, and in part by National Natural Science Foundation of China under Grant 62201181. The associate editor coordinating the review of this article and approving it for publication was Dr. Fathi Abdelmalek. *(Corresponding author: Guohua Liu.)*

The authors are with the School of Electronics and Information, Hangzhou Dianzi University, Hangzhou 310018, China (e-mail: yujianyuan@hdu.edu.cn; ghliu@hdu.edu.cn; zhiqun@hdu.edu.cn; 212040205@hdu.edu.cn; mh71828@hdu.edu.cn).

Digital Object Identifier 10.1109/JSEN.2022.3211566

LUT per measurement. However, in practical applications, the measurement of high loss of liquid materials is also a major problem. Therefore, Ebrahimi et al. [23] established the fluid channel above the CSRR gap. When this area resonates, a strong electric field generates an area that is very sensitive to the changes of nearby dielectric materials. The cross section of the fluid channel of the designed microfluidic sensor is as small as 0.06 × 0.70 mm. In [24], a circular multiring SRR microwave sensor with a working center frequency of 2.1 GHz is proposed, and the resonant frequency and its transmission coefficient are used to detect the complex dielectric constant of the liquid. The sample container of the sensor is a microcapillary made of glass material, which vertically passes through the outer ring groove of the sensor and uses a small volume of liquid (2.5 $\mu$L), and measurement can be realized. On the other hand, with the improvement of sensor sensitivity, the cross sensitivity also increases. Therefore, some temperature and humidity factors in the test environment are likely to affect the measurement results. The differential structure is a simple and practical method to eliminate environmental interference. Ebrahimi et al. [25] proposed a microwave sensor for detecting the water volume fraction in the glycerol–water solutions. The sensor is designed using a planar transmission line terminated with a series RLC resonator. Two identical sensing elements are designed and fabricated for a differential measurement. A high-sensitivity detection platform has been obtained based on the measurement of the cross-mode reflection coefficient between the test and reference ports. In [26], a differential permittivity sensor based on a pair of uncoupled microstrip lines is proposed. Each microstrip line is loaded with a sensing unit. The disadvantage of the sensor is that the four ports make the measurement more troublesome, and the fluid channel directly covers the whole particle, so there is a large loss of the LUT. In this article, a planar differential microfluidic sensor based on the OCSRR structure is designed. The OCSRR structure provides high edge electric field strength and reduces the number of capacitors in the sensor so that the resonant frequency is only affected by the capacitors that change with the complex dielectric constant of LUT, which greatly improves the sensitivity of the sensor. Moreover, the proposed sensor has only two ports: one is used as a reference port and the other is used to characterize the complex permittivity of the LUT, which reduces the manufacturing cost of the sensor and makes the detection more convenient. Section II introduces the structure of the proposed sensor and analyzes the working principle of the sensor. Section III puts forward the equivalent circuit model of the OCSRR structure sensor and verifies its correctness. In addition, this section also analyzes the influence of the center frequency on the sensitivity of the sensor. Section IV introduces the experimental results of the proposed sensor and its comparison with the previous work. Section V summarizes the main conclusions.

## II. Preparation Principle and Structure of Sensor

### A. Preparation Principle

The OCSRR structure was first proposed in [27]. Fig. 1 consists of two annular grooves hollowed out in a sheet of metal.

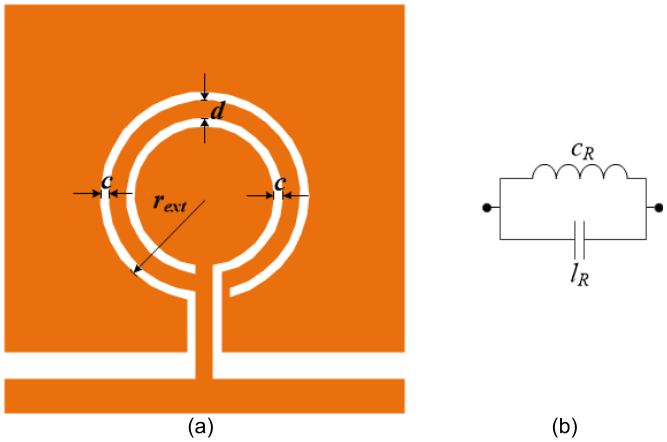


Fig. 1. (a) OCSRR structure proposed in [27]. (b) Its equivalent lumped-element circuit model. White represents the hollowed out part and orange represents the metal part.

Different from the CSRR structure, the OCSRR structure is directly connected to the microstrip line through the metal strips elongated outward at the gap of the ring, that is to say, the OCSRR is an open resonator, while the CSRR is a closed resonator. When a sensor is used, CSRR needs to be coupled to the microstrip line, but OCSRR does not. The inductance of the OCSRR particle is the inductance of the metal strip between the two annular grooves, and the capacitance mainly comes from the edge capacitance generated by the metal on both sides of the two annular grooves, which can be equivalent to a metal disk surrounded by a metal whose edge distance is $c$ fringing capacitance due to plane enclosing. The radius of the metal disk

$$r0 = r_{\text{ext}} - c - d/2. \tag{1}$$

Since the inductance of CSRR is one-quarter of the inductance of OCSRR, the resonant frequency of OCSRR is about half of the resonant frequency of CSRR. In the design of planar microfluidic sensors, the chosen resonant particles must be highly sensitive to the complex permittivity of the LUT loaded around the resonant particles. The outer annular groove of the OCSRR structure has a strong electric field, which makes the change of the complex permittivity of the LUT have a great impact on the dielectric properties of the resonant particles. Therefore, it is a good choice for designing planar microfluidic sensors. Moreover, the OCSRR structure is directly etched on the top layer of the dielectric plate, so there is no coupling capacitance with the ground, which is more suitable for making microfluidic sensors than CSRR. On the other hand, CSRR and transmission line transmit signals through coupling, which will result in low resonance depth, while the OCSRR transmits signals directly through the microstrip line, which is conducive to improving the sensitivity for distinguishing imaginary parts. The structure of the designed differential sensor is shown in Fig. 2. One OCSRR particle is loaded on each microstrip line. It should be noted that these two OCSRR particles are exactly the same, and their positions on the dielectric plate also need to be symmetric completely about the center line, so as to ensure the same change in the dielectric properties of the two particles when the same LUT

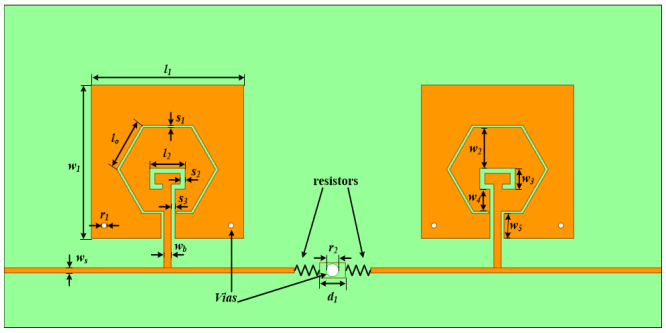


Fig. 2. Planar view of the proposed OCSRR-based sensor.

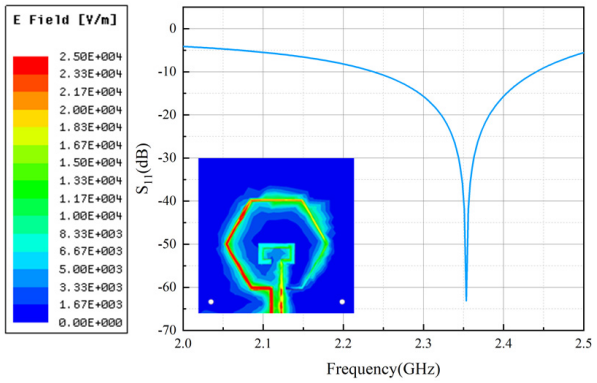


Fig. 3. Simulated transmission response of a bare sensor and the electric field distribution of OCSRR particles at the resonance frequency. The electric field strength of OCSRR particles at resonance frequency is marked on the left.

is added. The two ports output the reflection characteristics of two OCSRR particles: one of which is used to characterize the complex permittivity of the LUT and the other is used as a reference port. Since the two microstrip lines are grounded through the hole in the middle metal patch, the two metal sheets that etch the OCSRR particles leave a large distance, and there is no coupling between the two OCSRR particles.

## B. Structure of Sensor

The proposed sensor based on the OCSRR structure uses the dielectric plate of Rogers 4350B, with a thickness of 0.762 mm, a relative dielectric constant of 3.66, a loss tangent of 0.004, and a size of 20 × 52 mm. The width and length of the two microstrip lines are 0.4 and 23 mm, respectively. The designed sensor is used to characterize the complex dielectric constant of microfluidic samples and has high requirements for sensitivity. Therefore, the channel of fluid should be set at the position with the highest electric field intensity. The electric field intensity distribution is shown in the inset of Fig. 3. It can be found that there is a very dense electric field intensity on the side near the port of the outer annular groove of OCSRR particles. Therefore, put the fluid channel in this position. Microfluidic channels were fabricated using polydimethylsiloxane (PDMS). PDMS has electrical insulation, hydrophobicity, high shear resistance, and convenient processing. It is the best choice for making fluid channel. The cross-sectional area of the fabricated fluid channel is

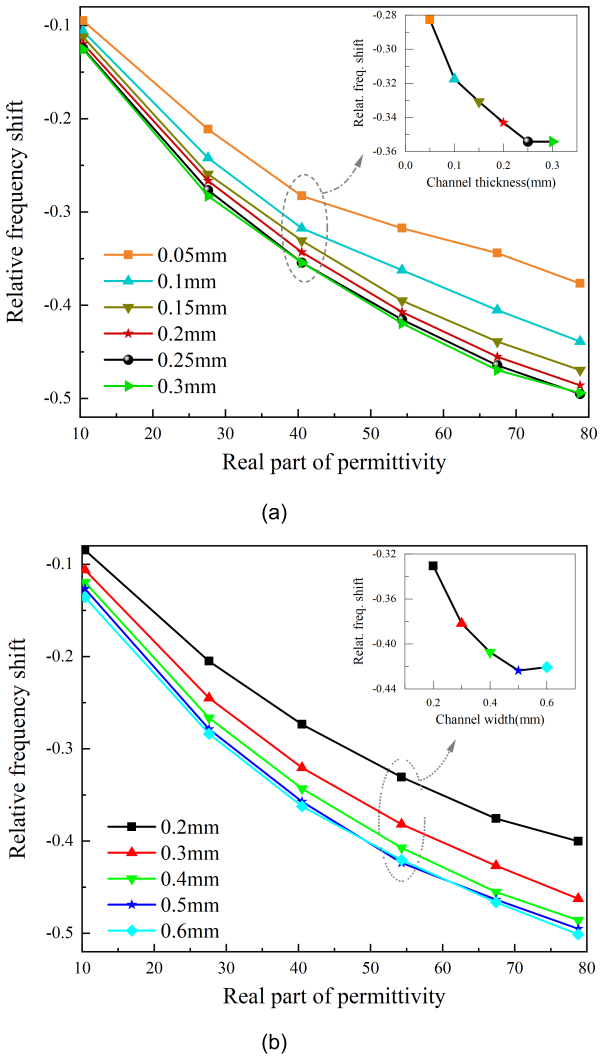


Fig. 4. Simulated relative frequency shift versus relative permittivity of the liquid sample for different (a) thicknesses and (b) widths of the microfluidic channel. The imaginary part of the LUT permittivity has been considered in the simulations.

0.4 × 0.2 mm, and the total length of the fluid channel is about 11 mm. The influence of the height and width of the fluid channel on the sensitivity is studied by simulation. The relative frequency shift is defined as the ratio of the frequency change to the resonant frequency of the no-load sensor. As shown in Fig. 4, the larger channel height and channel width make the LUT have a greater impact on the dielectric characteristics of the sensor, so as to obtain a higher relative frequency shift. However, it can be found that when the thickness of the fluid channel exceeds 0.2 mm and the width exceeds 0.4 mm, the increase of the relative frequency shift becomes very weak, which means that the area with the highest electric field intensity has almost been occupied by LUT. Therefore, in order to reduce the loss of LUT, it is worth giving up a small amount of sensitivity. The geometric parameters of the designed sensor are given in Table I.

Fig. 5 shows the simulation results of the proposed sensor. It can be seen that when the concentration of water is from 0% to 100%, the resonant frequency gradually decreases from 2.06 to 1.2 GHz, which is linear with the dielectric

TABLE I
GEOMETRICAL PARAMETERS OF THE PROPOSED SENSOR

| Parameter | $l_1$ | $l_2$ | $l_o$ | $w_1$ | $w_2$ | $w_3$ | $w_4$ | $w_5$ |
|---|---|---|---|---|---|---|---|---|
| Value(mm) | 12 | 2.8 | 4 | 12 | 3.1 | 1.6 | 1.6 | 2.3 |
| Parameter | $w_s$ | $w_b$ | $s_1$ | $s_2$ | $s_3$ | $r_1$ | $r_2$ | $d_1$ |
| Value(mm) | 0.4 | 0.6 | 0.2 | 0.4 | 0.3 | 0.4 | 1 | 2 |

TABLE II
EXTRACTED ELEMENT PARAMETERS OF THE EQUIVALENT CIRCUIT MODEL

| Channel 1/ Channel 2 | $L_p$ (nH) | $L_z$ (nH) | $C_p$ (pF) | $C_{LUT}$ (pF) | $C_{ref}$ (pF) | $R_{LUT}$ (Ω) | $R_{ref}$ (Ω) |
|---|---|---|---|---|---|---|---|
| Air/Air | 3.48 | 3.37 | 1.70 | 0 | 0 | 0 | 0 |
| Ethanol/ Ethanol | 3.48 | 3.37 | 1.70 | 0.55 | 0.55 | 5000 | 5000 |
| 50% Ethanol / Ethanol | 3.48 | 3.37 | 1.70 | 2.71 | 0.55 | 4989 | 5000 |

TABLE III
COMPARISON BETWEEN VARIOUS RESONANCE-BASED MICROWAVE MICROFLUIDIC SENSORS

| Ref | *Resonant type* | $f_0$(GHz) | $V$(μL) | $\Delta f$(MHz) | $S_{av}$(%) | *Diff.* |
|---|---|---|---|---|---|---|
| [29] | SIR | 1.91 | 0.39 | 349 | 0.45 | No |
| [23] | CSRR | 2.02 | 0.588 | 239 | 0.308 | No |
| [20] | MOCSRR | 0.33 | 80 | 60 | 0.85 | No |
| [32] | MCSRR | 1.618 | 5.4 | 520 | 0.626 | Yes |
| [34] | Shunt LC | 2.7 | 0.295 | 1050 | 1.61 | No |
| [35] | SRR | 1.156 | 10 | -- | -- | No |
| [36] | OLR | 2.6 | 5 | -- | 0.27 | No |
| [31] | MNG | 3.43 | 4.92 | 670 | 0.57 | No |
| T.W. | OCSRR | 2.35 | 0.91 | 820 | 0.882 | Yes |

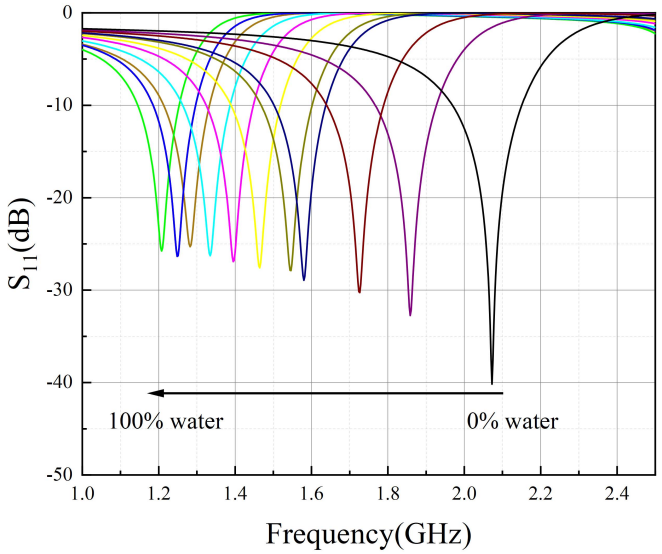


Fig. 5. Reflection coefficient of the proposed OCSRR-based sensor for different water volume fractions. The step water volume fraction is 10%.

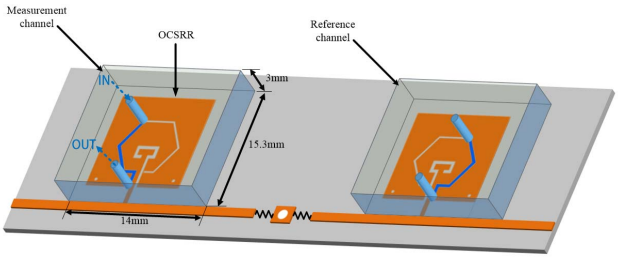


Fig. 6. Three-dimensional views of the designed microfluidic sensor with the PDMS microfluidic channels.

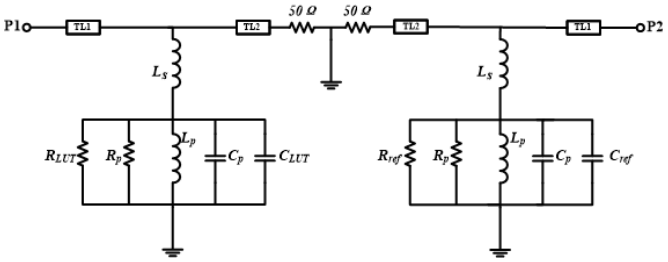


Fig. 7. Circuit model of the proposed sensor.

constant of water–ethanol solution. A 3-D view of the designed microfluidic sensor is shown in Fig. 6. Two microstrip lines are loaded with an OCSRR particle and grounded at the center of the dielectric plate. PDMS fluid channels of the same size are placed on the two OCSRR particles, and there is a considerable interval between the two particles so that there is no coupling between the two particles, and the structures on both sides are identical, ensuring that the reflection coefficients of the two resonators are completely consistent in the same environment among them. The OCSRR particle on the left is used for measurement, and the other is used as a reference. In this design, the OCSRR uses a hexagonal outer ring, which can effectively reduce the capacitance of the resonator itself at no-load and increase the influence of LUT on the resonant frequency. The rectangular inner ring makes it easier to adjust the position, so as to obtain the maximum electric field accumulation.

## III. CIRCUIT MODEL AND VALIDATION

The equivalent circuit of the proposed sensor is shown in Fig. 7. Among them, the short transmission line with $Z_C$ characteristic impedance represents the microstrip line on both sides of OCSRR particles. $L_s$ represents the inductance of the metal strip connecting OCSRR particles and microstrip lines. $L_P$, $C_P$, and $R_P$ represent the inductance, capacitance, and resistance of OCSRR particles, respectively. $C_{\mathrm{LUT}}$, $R_{\mathrm{LUT}}$, $C_{\mathrm{ref}}$, and $R_{\mathrm{ref}}$ simulate the changes of capacitance and resistance of the sensor when the LUT is added to the sensor. The resonant

frequency $f_Z$ of the sensor is

$$f_z = \frac{1}{2\pi\sqrt{L_p(C_p + C_{\mathrm{LUT}})}}. \tag{2}$$

The resonant frequency $f_0$ of the sensor under no-load is given as follows:

$$f_0 = \frac{1}{2\pi\sqrt{L_p \times C_p}}. \tag{3}$$

By observing the Smith chart with the $S_{11}$ parameter, we can obtain $f_r$ and the susceptance $B(\omega_r)$ as follows:

$$B(\omega_0) = \frac{\omega_0 L}{Z_0^2 + (\omega_0 L)^2} \tag{4}$$

where $\omega_0 = 2\pi f_0$ and $Z_0$ and $L$ are the characteristic impedance and inductance of the transmission lines on both sides of OCSRR particle, respectively. Moreover, when the phase of transmission coefficient is 90°, the series impedance $Z_r$ and shunt impedance $Z_k$ of the T-circuit model have the following relationship:

$$Z_0(\omega_{\pi/2}) = -Z_k(\omega_{\pi/2}) \tag{5}$$

where $\omega_{\pi/2} = 2\pi f_{\pi/2}$. Through the above formulas (3)–(5), the values of the lumped elements $C_P$ and $L_P$ can be calculated [28]. $L_s$ has no effect on the resonant frequency, it only represents the inductance of the metal strip connecting OCSRR particles and microstrip lines. Therefore, the value of $L_s$ can be calculated from the physical characteristics of the metal strip. Finally, using Keysight advanced design system (ADS) obtain the value of $R_p$, and fine-tuning other obtained values. According to the above analysis, the interesting parameters in the circuit model can be obtained.

### A. Validation

Since the inductance of OCSRR particles is mainly the metal inductance between two annular grooves, it is not affected by LUT. This inductance remains unchanged throughout the test process $L_Z$ as well. The capacitance and resistance of OCSRR particles will be affected by LUT, which is the working principle of the sensor.

In order to verify the accuracy of the equivalent circuit model, the following situations are considered. First, the channel is empty. Second, pure ethanol is added to both fluid channels. Third, pure ethanol is added to the fluid channel corresponding to the OCSRR particles as a reference, and a 50% ethanol solution is added to the other fluid channel. The reflection coefficients and their phases of the above three cases are obtained by simulation (see Table II), and the circuit parameters in the equivalent circuit model in Fig. 7 are obtained through the parameter extraction method in [22] (see Table II). Fig. 8 shows the response of the sensor under no-load. There is good agreement between the simulation results of the circuit model and the simulation results of the physical model in high frequency structure simulator (HFSS). When pure ethanol is added into the two fluid channels at the same time, the results obtained are shown in Fig. 9. At this time, the extracted circuit parameters have been applied to the model. It can be found that $L_Z$ and $L_P$ remain unchanged, while the capacitance and

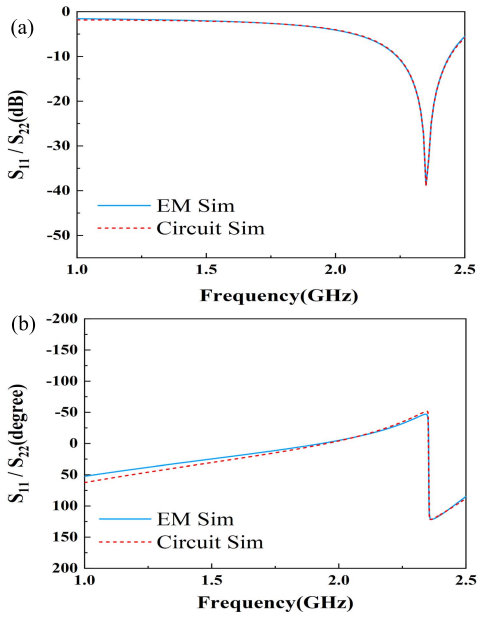


Fig. 8. Reflection coefficient of the proposed OCSRR-based sensor loaded with empty channel. (a) Magnitude. (b) Phase.

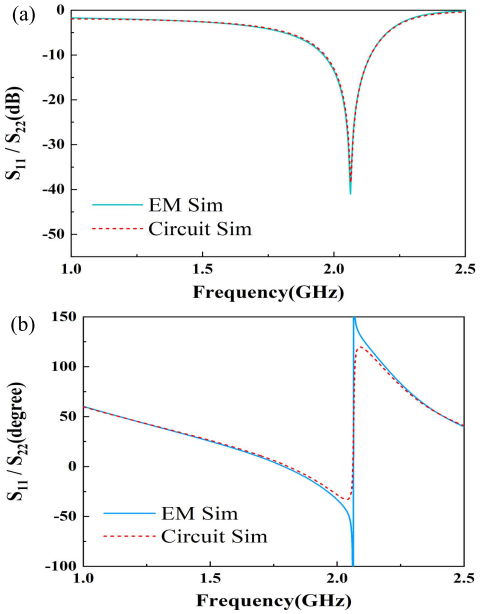


Fig. 9. Reflection coefficient of the proposed OCSRR-based sensor loaded with ethanol. (a) Magnitude. (b) Phase.

resistance change. This result confirms the conclusion that the loaded liquid will not affect the inductance of OCSRR particles but will affect the capacitance and resistance of OCSRR particles. As shown in Fig. 10, when pure ethanol is added to the fluid channel corresponding to port 2 and a 50% ethanol solution is added to the other fluid channel, the results obtained in $S_{11}$ are consistent with those in the second case, and $S_{22}$ changes, which shows that the two resonators do not interfere with each other, which supports the reliability of the differential sensor.

### B. Sensitivity Analysis

The proposed sensor is used to extract the dielectric constant of LUT, so it is very important to improve the sensitivity of

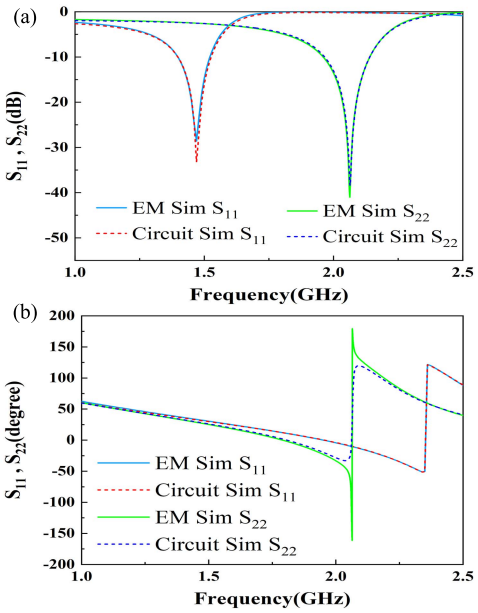


Fig. 10. Reflection coefficient of the proposed OCSRR-based sensor loaded with ethanol and 50% ethanol. (a) Magnitude. (b) Phase.

the sensor. The sensitivity is defined as

$$S = \frac{\Delta f_z}{\Delta \varepsilon} \tag{6}$$

where $\Delta f_z$ is the shift in the resonant frequency and $\Delta \varepsilon$ is the change in the permittivity of the dielectric sample loaded on the resonator. When considering that the increase of no-load frequency may increase $\Delta f_z$, the definition of sensitivity can be modified as

$$S = \frac{\Delta f_z}{\Delta \varepsilon} \times \frac{1}{f_{\text{empty}}} \tag{7}$$

where $f_{\text{empty}}$ represents the resonant frequency when the fluid channel is empty. When the LUT is loaded in the fluid channel, it is equivalent to adding an additional capacitor $C_{\text{LUT}}$ to the sensor (only the real dielectric constant is discussed here), so the resonant frequency changes from $f_0$ at no-load to $f_z$, that is, $\Delta f_z$ is shifted; from (2), (3), and (7), (8) can be obtained

$$S = \frac{f_z}{\Delta \varepsilon}\left(1 - \sqrt{\frac{1}{1 + \frac{C_{\text{LUT}}}{C_R}}}\right) \times \frac{1}{f_{\text{empty}}} \tag{8}$$

where $\Delta \varepsilon$ and $C_{\text{LUT}}$ are determined by LUT. However, $f_z$ and $C_R$ are only determined by the physical properties of the sensor. Therefore, $f_z$ and $C_R$ are the key to control sensitivity when designing sensors. It is not difficult to find that when $f_z$ and $C_R$ increase, the sensitivity also increases. However, when increasing $f_z$, we need to consider the improvement of measurement difficulty and processing difficulty. When raising $C_R$, it is necessary to consider the influence of the capacitance of the part of the OCSRR outer ring without LUT with low electric field strength on the sensitivity. Therefore, a more appropriate value of $f_z$ and $C_R$ must be obtained through various considerations.

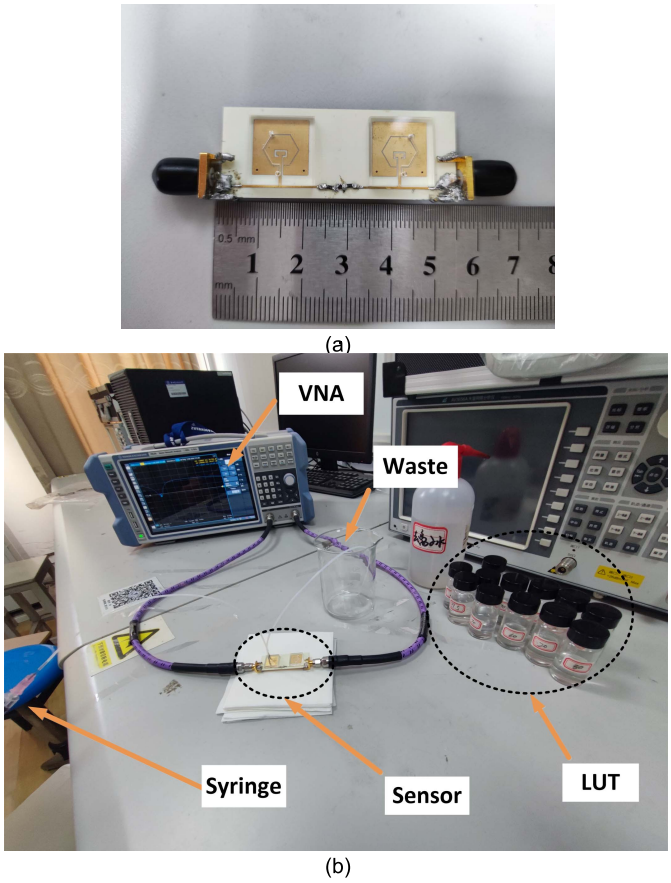


Fig. 11. Photographs of (a) fabricated sensors and (b) experimental setup.

## IV. Experimental Results and Analysis

Because the water–ethanol binary solution provides a wide range of complex permittivity, this article uses the proposed microfluidic sensor to extract the complex permittivity of the water–ethanol binary solution to prove the practicability of the proposed microfluidic sensor. The real part of the complex permittivity is characterized by the resonant frequency, whereas the imaginary part of the complex permittivity can be characterized by the change of the resonant depth of the sensor based on the OCSRR structure. As shown in Fig. 11, a pair of standard subminiature version A (SMA) connectors interfaces are installed on the microstrip line. The reflection coefficient $S_{11}$ obtained at the left port is used to characterize the complex dielectric constant of LUT, and the reflection coefficient $S_{22}$ obtained at the right port is used as the reference. Prepare water–ethanol binary solutions of different concentrations with a gradient of 10% and store them in small bottles. Connect port 1 of vector network analyzer (VNA) to port 1 of the sensor and port 2 of VNA to port 2 of the sensor. Then, connect the PDMS fluid channel to OCSRR particles. Then, use a syringe to input water–ethanol binary solutions of different concentrations into the fluid channel. After each extraction, the fluid channel shall be cleaned and dried with a hot air blower to prevent the residual liquid from interfering with the next measurement. In addition, in order to avoid liquid overflowing the PDMS fluid channel, the pressure of injecting liquid into

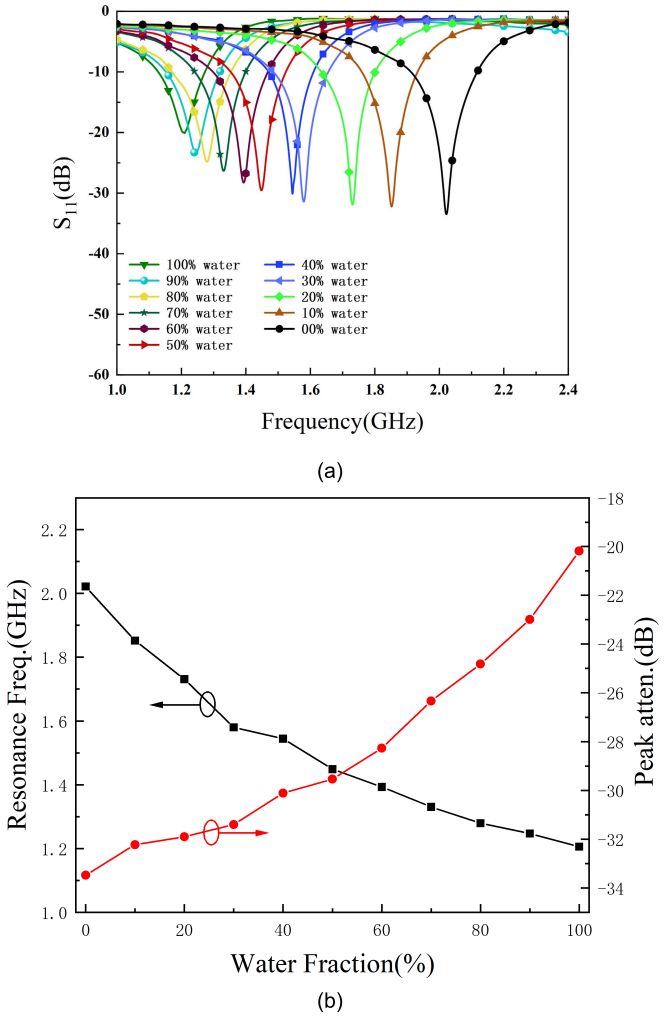


Fig. 12. (a) Measured sensor responses to the ethanol–water mixture with different fractions of water. (b) Resonance frequency and the peak attenuation for different water volume fractions.

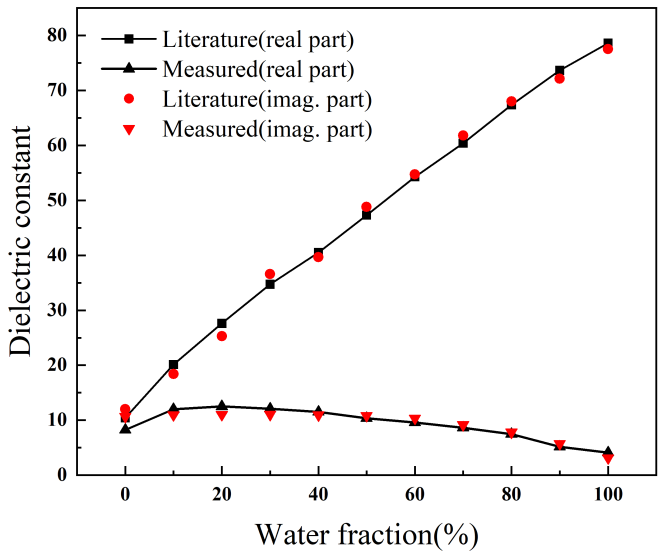


Fig. 13. Comparison between the actual value of the relative permittivity from [30] and the ones measured using the designed sensor.

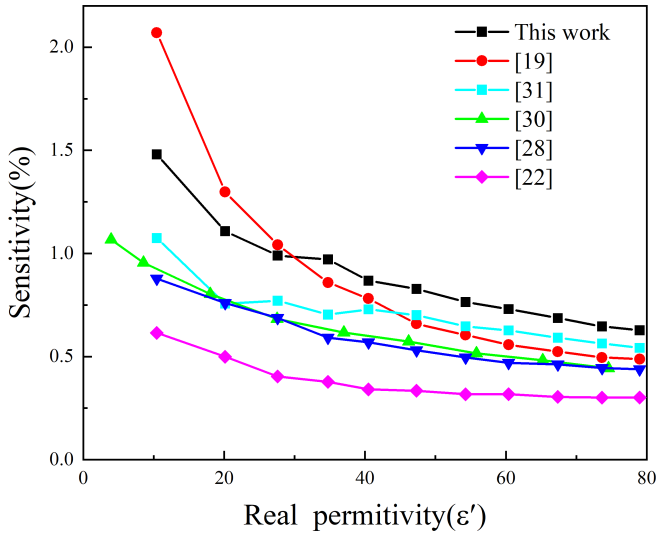


Fig. 14. Comparison between the sensitivity of the proposed design and the state-of-the-art devices based on the measured results.

the channel during measurement shall not exceed 300 mbar [29]. Fig. 12(a) shows the reflection coefficient of the proposed OCSRR-based sensor at different water volume fractions. Obviously, the resonant frequency decreases from 2.05 to 1.22 GHz with the increase of water volume fraction, the frequency shift exceeds 800 MHz, and the resonant amplitude also changes with the water volume fraction, which is related to the imaginary part of the complex dielectric constant of LUT. The resonance frequency and peak attenuation extracted from the measurements are plotted in Fig. 12(b). In order to describe the relationship between the change of resonant frequency and peak attenuation as a function of the change of complex dielectric constant, the nonlinear least-squares curve fitting is used, and an equation is derived as

$$\varepsilon'_{\mathrm{LUT}} = 66.0773 f_z^2 - 293.5280 f_z + 335.3873 \tag{9}$$

$$\varepsilon''_{\mathrm{LUT}} = -0.078(S_{11}(\mathrm{dB}))^2 - 4.8779 S_{11}(\mathrm{dB}) - 65.1899 \tag{10}$$

where $\varepsilon'_{\mathrm{LUT}}$ represents the real part of the dielectric constant of LUT, $\varepsilon''_{\mathrm{LUT}}$ represents the imaginary part of the dielectric constant of LUT, and $S_{11}(\mathrm{dB})$ represents the amplitude of $S_{11}$ corresponding to the resonant frequency. The reference sample is the air. The complex permittivity of the water–ethanol solution at their resonance frequencies is extracted from [30].

In order to verify the accuracy of the mathematical model developed in (9) and (10), the ethanol aqueous solution with a concentration ranging from 0% to 100% was repeatedly measured three times, and the average value was compared with the actual ones obtained from [30]. As shown in Fig. 13, it is found that the measured values are very consistent with the actual values obtained from [30], which verifies the accuracy of the mathematical model developed in (9) and (10).

Finally, compare the sensor proposed in this article with similar sensors proposed recently in terms of various parameters to more clearly show the advantages of the designed sensor. The sensitivity of a microfluidic sensor based on resonance is defined as

$$S_{\varepsilon'_r} = \frac{\left|f_{\varepsilon'_r} - f_{\mathrm{empty}}\right|}{f_{\mathrm{empty}}} \times \frac{1}{\varepsilon'_r - 1} \times 100 \tag{11}$$

where $f_{\varepsilon_r'}$ is the resonance frequency for the solution with $\varepsilon_r'$. Table III summarizes the resonant type, resonant frequency, liquid sample volume, frequency offset, and average sensitivity of the proposed sensors and previous designs. Fig. 14 shows the difference in average sensitivity between the sensors proposed in this article and similar sensors proposed recently. Lee et al. [20] used a concentrated electric field structure to better concentrate on the electric field in a rectangular area and used the FR4 dielectric plate to make a liquid container. This design not only improves the sensitivity but also reduces the manufacturing cost of the sensor. However, the sensor consumes too much LUT. Ebrahimi et al. [23] adopted the PDMS channel, which greatly reduces the consumption of LUT, but the sensitivity is low. The sensor proposed in [31] uses a stepped impedance resonators (SIRs) structure and improves the sensitivity by opening a slot in the ground plane below the resonator to eliminate the parasitic capacitance contribution of the metallization of the resonator. Its sensitivity still needs to be improved. In [32], a square spiral metamaterial structure is used, which helps to achieve significant compactness of the equipment and establish significant sensitivity in a small cross-sectional area. Although its sensitivity has been further improved, it still consumes a lot of LUT. A differential CSRR structure is proposed in [33], which is similar to [32] in sensitivity and invasiveness. An ultrahigh-sensitivity microfluidic sensor is designed by using a series-connected shunt *LC* resonator in [34]. It achieves very high sensitivity by eliminating any additional capacitance that does not affect the sensing mechanism and only retaining the gap capacitance between triangular patches on the top of the medium. However, it still does not consider the impact of environmental factors. Abdolrazzaghi et al. [35] using an active SRR designed a high-Q microwave sensor device for noninvasive real-time measurement of glucose in media containing serum that approximates human interstitial fluid. Although its loss is compensated to enhance the quality factor, its measurement convenience has declined. Abdolrazzaghi et al. [36] proposed a microwave sensor based on open-loop resonators (OLRs). Its dispersion is engineered to enable a wide frequency range supporting transmission resonances of the LUT-loaded resonator. However, it still consumes more LUT per measurement than this design. The sensor based on OCSRR proposed in this article still keeps the liquid consumption within 1 $\mu$L and greatly improves the sensitivity on this basis. Moreover, the differential structure can eliminate the influence of environmental factors on the measurement, making the measurement results more reliable. The proposed sensor is also small in size and suitable for carrying and integration. In summary, the proposed sensor shows very competitive performance in comparison with the others.

## V. Conclusion

In conclusion, a novel planar microfluidic sensor is proposed in this article. The complex permittivity of the LUT is recovered by loading the exact same OCSRR structure on a pair of uncoupled microstrip lines. Fluid channels were added to both OCSRR structures: one channel was injected with deionized water as a reference and the other fluid channel was injected with LUT to characterize its complex permittivity. A prototype of the sensor was fabricated and used to recover the complex permittivity of water–ethanol mixtures of different concentrations. The experimental results show that the two sensing units in the sensor do not interfere with each other, which can effectively suppress the test errors caused by environmental factors (humidity, temperature, and so on), and the simulation results are in good agreement with the measured results. The sensor achieves a high sensitivity of 0.882% on average. The low cost, miniaturization, and noninvasive advantages of this sensor make it promising for industrial production.

## References


[1] S. Gabriel, R. W. Lau, and C. Gabriel, "The dielectric properties of biological tissues: II. Measurements in the frequency range 10 Hz to 20 GHz," *Phys. Med. Biol.*, vol. 41, no. 11, p. 2251, Nov. 1996.

[2] A. Tamra, D. Dubuc, M. Rols, and K. Grenier, "Microwave monitoring of single cell monocytes subjected to electroporation," *IEEE Trans. Microw. Theory Techn.*, vol. 65, no. 9, pp. 3512–3518, Sep. 2017.

[3] A. A. Abduljabar, N. Clark, J. Lees, and A. Porch, "Dual mode microwave microfluidic sensor for temperature variant liquid characterization," *IEEE Trans. Microw. Theory Techn.*, vol. 65, no. 7, pp. 2572–2582, Jul. 2017.

[4] J.-K. Park et al., "Real-time humidity sensor based on microwave resonator coupled with PEDOT: PSS conducting polymer film," *Sci. Rep.*, vol. 8, no. 1, pp. 1–8, 2018.

[5] J. Naqui, M. Durán-Sindreu, and F. Martín, "Alignment and position sensors based on split ring resonators," *Sensors*, vol. 12, no. 9, pp. 11790–11797, Aug. 2012.

[6] J. Naqui and F. Martín, "Transmission lines loaded with bisymmetric resonators and their application to angular displacement and velocity sensors," *IEEE Trans. Microw. Theory Techn.*, vol. 61, no. 12, pp. 4700–4713, Dec. 2013.

[7] M. R. Islam et al., "Tri circle split ring resonator shaped metamaterial with mathematical modeling for oil concentration sensing," *IEEE Access*, vol. 9, pp. 161087–161102, 2021.

[8] M. S. Boybay and O. M. Ramahi, "Material characterization using complementary split-ring resonators," *IEEE Trans. Instrum. Meas.*, vol. 61, no. 11, pp. 3039–3046, Nov. 2012.

[9] W. Withayachumnankul, K. Jaruwongrungsee, A. Tuantranont, C. Fumeaux, and D. Abbott, "Metamaterial-based microfluidic sensor for dielectric characterization," *Sens. Actuators A, Phys.*, vol. 189, pp. 233–237, Jan. 2013.

[10] M. C. Jain, A. V. Nadaraja, B. M. Vizcaino, D. J. Roberts, and M. H. Zarifi, "Differential microwave resonator sensor reveals glucose-dependent growth profile of *E. Coli* on solid agar," *IEEE Microw. Wireless Compon. Lett.*, vol. 30, no. 5, pp. 531–534, May 2020.

[11] S. Mohammadi, K. K. Adhikari, M. C. Jain, and M. H. Zarifi, "High-resolution, sensitivity-enhanced active resonator sensor using substrate-embedded channel for characterizing low-concentration liquid mixtures," *IEEE Trans. Microw. Theory Techn.*, vol. 70, no. 1, pp. 576–586, Jan. 2022.

[12] P. Vélez, L. Su, K. Grenier, J. Mata-Contreras, D. Dubuc, and F. Martín, "Microwave microfluidic sensor based on a microstrip splitter/combiner configuration and split ring resonators (SRRs) for dielectric characterization of liquids," *IEEE Sensors J.*, vol. 17, no. 20, pp. 6589–6598, Aug. 2017.

[13] K. T. M. Shafi, M. A. H. Ansari, A. K. Jha, and M. J. Akhtar, "Design of SRR-based microwave sensor for characterization of magnetodielectric substrates," *IEEE Microw. Compon. Lett.*, vol. 27, no. 5, pp. 524–526, May 2017.

[14] J. Mata-Contreras, C. Herrojo, and F. Martín, "Application of split ring resonator (SRR) loaded transmission lines to the design of angular displacement and velocity sensors for space applications," *IEEE Trans. Microw. Theory Techn.*, vol. 65, no. 11, pp. 4450–4460, Nov. 2017.

[15] N. Kazemi, M. Abdolrazzaghi, and P. Musilek, "Comparative analysis of machine learning techniques for temperature compensation in microwave sensors," *IEEE Trans. Microw. Theory Techn.*, vol. 69, no. 9, pp. 4223–4236, Sep. 2021.

[16] C.-S. Lee and C.-L. Yang, "Complementary split-ring resonators for measuring dielectric constants and loss tangents," *IEEE Microw. Wireless Compon. Lett.*, vol. 24, no. 8, pp. 563–565, Aug. 2014.

[17] S. A. Alotaibi, Y. Cui, and M. M. Tentzeris, "CSRR based sensors for relative permittivity measurement with improved and uniform sensitivity throughout [0.9–10.9] GHz band," *IEEE Sensors J.*, vol. 20, no. 9, pp. 4667–4678, May 2020.
[18] M. Saadat-Safa, V. Nayyeri, M. Khanjarian, M. Soleimani, and O. M. Ramahi, "A CSRR-based sensor for full characterization of magneto-dielectric materials," *IEEE Trans. Microw. Theory Techn.*, vol. 67, no. 2, pp. 806–814, Feb. 2019.
[19] J. G. D. Oliveira, E. N. M. G. Pinto, V. P. Silva Neto, and A. G. D'Assunção, "CSRR-based microwave sensor for dielectric materials characterization applied to soil water content determination," *Sensors*, vol. 20, no. 1, p. 255, Jan. 2020.
[20] C. Lee, B. Bai, Q. Song, Z. Wang, and G. Li, "Open complementary split-ring resonator sensor for dropping-based liquid dielectric characterization," *IEEE Sensors J.*, vol. 19, no. 24, pp. 11880–11890, Dec. 2019.
[21] A. E. Omer et al., "Multiple-cell microfluidic dielectric resonator for liquid sensing applications," *IEEE Sensors J.*, vol. 21, no. 5, pp. 6094–6104, Mar. 2021.
[22] N. K. Tiwari, S. P. Singh, and M. J. Akhtar, "Novel improved sensitivity planar microwave probe for adulteration detection in edible oils," *IEEE Microw. Wireless Compon. Lett.*, vol. 29, no. 2, pp. 164–166, Feb. 2019.
[23] A. Ebrahimi, W. Withayachumnankul, S. Al-Sarawi, and D. Abbott, "High-sensitivity metamaterial-inspired sensor for microfluidic dielectric characterization," *IEEE Sensors J.*, vol. 14, no. 5, pp. 1345–1351, May 2014.
[24] M. R. Islam et al., "Metamaterial sensor based on rectangular enclosed adjacent triple circle split ring resonator with good quality factor for microwave sensing application," *Sci. Rep.*, vol. 12, no. 1, pp. 1–18, Dec. 2022.
[25] A. Ebrahimi et al., "Differential microwave sensor for characterization of glycerol–water solutions," *Sens. Actuators B, Chem.*, vol. 321, Oct. 2020, Art. no. 128561.
[26] P. Vélez, K. Grenier, J. Mata-Contreras, D. Dubuc, and F. Martín, "Highly-sensitive microwave sensors based on open complementary split ring resonators (OCSRRs) for dielectric characterization and solute concentration measurement in liquids," *IEEE Access*, vol. 6, pp. 48324–48338, 2018.
[27] A. Velez, F. Aznar, J. Bonache, M. C. Velazquez-Ahumada, J. Martel, and F. Martin, "Open complementary split ring resonators (OCSRRs) and their application to wideband CPW band pass filters," *IEEE Microw. Wireless Compon. Lett.*, vol. 19, no. 4, pp. 197–199, Apr. 2009.
[28] A. Ebrahimi, W. Withayachumnankul, S. F. Al-Sarawi, and D. Abbott, "Dual-mode behavior of the complementary electric-LC resonators loaded on transmission line: Analysis and applications," *J. Appl. Phys.*, vol. 116, no. 8, 2014, Art. no. 083705.
[29] L.-C. Fan, W.-S. Zhao, D.-W. Wang, Q. Liu, S. Chen, and G. Wang, "An ultrahigh sensitivity microwave sensor for microfluidic applications," *IEEE Microw. Wireless Compon. Lett.*, vol. 30, no. 12, pp. 1201–1204, Dec. 2020.
[30] J.-Z. Bao, M. L. Swicord, and C. C. Davis, "Microwave dielectric characterization of binary mixtures of water, methanol, and ethanol," *J. Chem. Phys.*, vol. 104, no. 12, pp. 4441–4450, 1996.
[31] A. Ebrahimi, J. Scott, and K. Ghorbani, "Ultrahigh-sensitivity microwave sensor for microfluidic complex permittivity measurement," *IEEE Trans. Microw. Theory Techn.*, vol. 67, no. 10, pp. 4269–4277, Oct. 2019.
[32] S. Kayal, T. Shaw, and D. Mitra, "Design of metamaterial-based compact and highly sensitive microwave liquid sensor," *Appl. Phys. A, Solids Surf.*, vol. 126, no. 1, pp. 1–9, Jan. 2020.
[33] H. Y. Gan, W. S. Zhao, Q. Liu, D. W. Wang, L. X. Dong, and G. F. Wang, "Differential microwave microfluidic sensor based on microstrip complementary split-ring resonator (MCSRR) structure," *IEEE Sensors J.*, vol. 20, no. 11, pp. 5876–5884, Jun. 2020.
[34] H. Abdelwahab, A. Ebrahimi, F. J. Tovar-Lopez, G. Beziuk, and K. Ghorbani, "Extremely sensitive microwave microfluidic dielectric sensor using a transmission line loaded with shunt LC resonators," *Sensors*, vol. 21, no. 20, p. 6811, Oct. 2021.
[35] M. Abdolrazzaghi, N. Katchinskiy, A. Y. Elezzabi, P. E. Light, and M. Daneshmand, "Noninvasive glucose sensing in aqueous solutions using an active split-ring resonator," *IEEE Sensors J.*, vol. 21, no. 17, pp. 18742–18755, Sep. 2021.
[36] M. Abdolrazzaghi, M. Daneshmand, and A. K. Iyer, "Strongly enhanced sensitivity in planar microwave sensors based on metamaterial coupling," *IEEE Trans. Microw. Theory Techn.*, vol. 66, no. 4, pp. 1843–1855, Apr. 2018.

**Jianyuan Yu** received the B.E. degree from Shaoxing University, Shaoxing, China, in 2021. He is currently pursuing the M.S. degree with Hangzhou Dianzi University, Hangzhou, China.

His research interest is focused on the design of microwave sensors and RF communication circuits.

**Guohua Liu** received the M.S. degree from East China Normal University, Shanghai, China, in 2004, and the Ph.D. degree in electronic science and technology from Hangzhou Dianzi University (HDU), Hangzhou, China, in 2020.

He is currently a Professor with HDU. His research interests include microwave circuits, sensors, antennas, and wireless systems design.

**Zhiqun Cheng** (Member, IEEE) received the B.S. and M.S. degrees from the Hefei University of Technology, Hefei, China, in 1986 and 1995, respectively, and the Ph.D. degree in microelectronics and solid-state electronics from the Shanghai Institute of Metallurgy, Chinese Academy of Sciences, Shanghai, China, in 2000.

From 1986 to 1997, he was a Teaching Assistant and a Lecturer with the Hefei University of Technology. From 2000 to 2005, he was an Associate Professor with the Shanghai Institute of Metallurgy, Chinese Academy of Sciences. He is currently a Professor and the Dean of the School of Electronic and Information, Hangzhou Dianzi University, Hangzhou, China. He has authored or coauthored over 150 technical journals and conference papers. His research interests include microwave theory and technology, monolithic microwave integrated circuit (MMIC), power amplifiers, and RF front end.

Dr. Cheng is currently a member of the Council of Zhejiang Electronic Society. He was also the Chair of the Organizational Committee for over ten international conferences.

**Yu Song** received the B.E. degree from the North China University of Water Resources and Electric Power, Zhengzhou, China, in 2021. He is currently pursuing the M.S. degree with Hangzhou Dianzi University, Hangzhou, China.

His research interests include the design of RF communication circuits.

**Minghui You** received the B.E. degree in electronic and information engineering from the Chengdu University of Technology, Chengdu, China, in 2020. He is pursuing the M.S. degree with Hangzhou Dianzi University, Hangzhou, China.

His current research interests include Doherty power amplifiers, substrate integrated waveguides, and load-modulated balanced power amplifiers.